Space Weather

RESEARCH ARTICLE
10.1029/2019SW002269

Special Section:
Scientific Challenges of Space Weather Forecasting Including Extremes

Temporal and Spatial Evolutions of a Large Sunspot Group and Great Auroral Storms Around the Carrington Event in 1859

Hisashi Hayakawa[1,2], Yusuke Ebihara[3,4], David M. Willis[2,5], Shin Toriumi[6], Tomoya Iju[7], Kentaro Hattori[8], Matthew N. Wild[2], Denny M. Oliveira[9,10], Ilaria Ermolli[11], José R. Ribeiro[12], Ana P. Correia[12], Ana I. Ribeiro[13,14], and Delores J. Knipp[15,16]

[1]Graduate School of Letters, Osaka University, Toyonaka, Japan, [2]UK Solar System Data Centre, Space Physics and Operations Division, RAL Space, Science and Technology Facilities Council, Rutherford Appleton Laboratory, Didcot, UK, [3]Research Institute for Sustainable Humanosphere, Kyoto University, Uji, Japan, [4]Unit of Synergetic Studies for Space, Kyoto University, Kyoto, Japan, [5]Centre for Fusion, Space and Astrophysics, Department of Physics, University of Warwick, Coventry, UK, [6]Institute of Space and Astronautical Science (ISAS), Japan Aerospace Exploration Agency (JAXA), Sagamihara, Japan, [7]National Astronomical Observatory of Japan, Mitaka, Japan, [8]Graduate School of Science, Kyoto University, Kyoto, Japan, [9]Goddard Planetary Heliophysics Institute, University of Maryland, Baltimore County, Baltimore, MD, USA, [10]NASA Goddard Space Flight Center, Greenbelt, MD, USA, [11]INAF Osservatorio Astronomico di Roma, Monte Porzio Catone, Italy, [12]Departamento de Matemática e Ciências Experimentais, Escola Secundária Henrique Medina, Esposende, Portugal, [13]EPIUnit—Instituto de Saúde Pública, Universidade do Porto Rua das Taipas, Porto, Portugal, [14]Departamento de Ciências da Saúde Pública e Forenses e Educação Médica, Faculdade de Medicina, Universidade do Porto, Porto, Portugal, [15]High Altitude Observatory, National Center for Atmospheric Research, Boulder, CO, USA, [16]Smead Aerospace Engineering Sciences Department, University of Colorado Boulder, Boulder, CO, USA

Key Points:
- Original sunspot drawings during the 1859 storms are revealed and analyzed
- New auroral reports from Eurasia and Oceania fill the spatial and temporal gaps of the auroral visibility during the 1859 storms
- The 1859 storms are compared and contextualized with the other extreme space weather events

Supporting Information:
- Supporting Information S1

Correspondence to:
H. Hayakawa,
hayakawa@kwasan.kyoto-u.ac.jp
hisashi.hayakawa@stfc.ac.uk

Citation:
Hayakawa, H., Ebihara, Y., Willis, D. M., Toriumi, S., Iju, T., Hattori, K., et al (2019). Temporal and spatial evolutions of a large sunspot group and great auroral storms around the Carrington event in 1859. *Space Weather*, *17*, 1553–1569. https://doi.org/10.1029/2019SW002269

Received 3 JUN 2019
Accepted 14 AUG 2019
Accepted article online 29 AUG 2019
Published online 19 NOV 2019

Abstract The Carrington event is considered to be one of the most extreme space weather events in observational history within a series of magnetic storms caused by extreme interplanetary coronal mass ejections from a large and complex active region that emerged on the solar disk. In this article, we study the temporal and spatial evolutions of the source sunspot active region and visual aurorae and compare this storm with other extreme space weather events on the basis of their auroral spatial evolution. Sunspot drawings by Schwabe, Secchi, and Carrington describe the position and morphology of the source active region at that time. Visual auroral reports from the Russian Empire, Iberia, Ireland, Oceania, and Japan fill the spatial gap of auroral visibility and revise the time series of auroral visibility in middle to low magnetic latitudes. The reconstructed time series is compared with magnetic measurements and shows the correspondence between low-latitude to mid-latitude aurorae and the phase of magnetic storms. The spatial evolution of the auroral oval is compared with those of other extreme space weather events in 1872, 1909, 1921, and 1989 as well as their storm intensity and contextualizes the Carrington event, as one of the most extreme space weather events, but likely not unique.

Plain Language Summary The Carrington event is considered to be one of the most extreme space weather events in observational history. In this article, we have studied the temporal and spatial evolutions of the source active region and visual low-latitude aurorae. We have also compared this storm with other extreme space weather events on the basis of the spatial evolution. We have compared the available sunspot drawings to reconstruct the morphology and evolution of sunspot groups at that time. We have surveyed visual auroral reports in the Russian Empire, Ireland, Iberian Peninsula, Oceania, and Japan and fill the spatial gap of auroral visibility and revised its time series. We have compared this time series with magnetic measurements and shown the correspondence between low-latitude to midlatitude aurorae and the phase of magnetic storms. We have compared the spatial evolution of the auroral oval with those of other extreme space weather events in 1872, 1909, 1921, and 1989 as well as their storm intensity and concluded that the Carrington event is one of the most extreme space weather events but is likely not unique.

1. Introduction

After the earliest datable observation of a white-light flare in a large sunspot group by Carrington (1859) and Hodgson (1859) on 1 September 1859, humanity experienced one of the most extreme magnetic storms in

observational history (Cliver & Dietrich, 2013; Tsurutani et al., 2003). The reported white-light solar flare was followed by a sudden ionospheric disturbance, namely, a large magnetic crochet ≈110 nT (Boteler, 2006; Stewart, 1861), which suggests the flare intensity as ≈X45—one of the largest in observational history and comparable to the largest modern flare on 4 November 2003 (Boteler, 2006; Cliver & Dietrich, 2013; Curto et al., 2016; see also Thomson et al., 2004).

The Carrington event has been thus considered a benchmark of extreme space weather events in terms of its sudden ionospheric disturbance, solar energetic particles, solar wind velocity, magnetic disturbance, and equatorward boundary of auroral display (Cliver & Svalgaard, 2004). We note that recent discussions on the ice core data (e.g., Mekhaldi et al., 2018; Schrijver et al., 2012; Sukhodolov et al., 2017; Usoskin & Kovaltsov, 2012; Wolff et al., 2012) made the existing estimate of its solar energetic particle fluence (e.g., McCracken et al., 2001; Shea et al., 2006; Smart et al., 2006) rather controversial (Cliver & Dietrich, 2013; Usoskin & Kovaltsov, 2012; Usoskin, 2017).

This great magnetic storm is characterized by an extreme negative magnetic excursion. For example, a value of ≈ −1,600 nT was measured at Bombay (N18°56′, E072°50′; Tsurutani et al., 2003). The anomalously short duration of the negative magnetic excursion has attracted much attention with regard to its cause in relation to the equatorward boundary of auroral visibility, ≈23° (Tsurutani et al., 2003) versus ≈18° (Green & Boardsen, 2006) in magnetic latitude (MLAT). The current source of the large-amplitude magnetic disturbance is also a matter of controversy. One possible source is the enhanced ring current (Tsurutani et al., 2003; Li et al., 2006; Keika et al., 2015; see also Daglis et al., 1999), one is the auroral electrojet (Akasofu & Kamide, 2018; Cliver & Dietrich, 2013; Green & Boardsen, 2006), and another is field-aligned current (Cid et al., 2014, 2015).

Another characteristic of this event was the great auroral displays down to middle to low MLATs (e.g., Green & Boardsen, 2006; Ribeiro et al., 2011; Hayakawa, Ebihara, Hand, et al., 2018). The temporal and spatial evolutions of auroral visibility were compared with the location of the magnetic record at Bombay by Green and Boardsen (2006). Their auroral records were concentrated in the Western Hemisphere. The equatorward boundary of the auroral oval reconstructed from the contemporary observational reports was as low as ≈28.5°/30.8° invariant latitude (ILAT; Hayakawa, Ebihara, Hand, et al., 2018). Note that ILAT signifies a parameter for the magnetic field line, along which electrons move and cause auroral brightening (Hayakawa, Ebihara, Hand, et al., 2018; O'Brien et al., 1962).

The auroral visibility around the Eurasian continent remains largely unexamined, except for the records in Western Europe and East Asia (e.g., Green & Boardsen, 2006; Hayakawa, Ebihara, Hand, et al., 2018; Kimball, 1960). Since the magnetic disturbances depend on magnetic local time, the simultaneous observations of the magnetic disturbances and the auroral visibilities provide a better understanding of the Carrington event. Thus, it is of significant interest to revise the temporal and spatial evolutions of the auroral oval during the stormy interval around the Carrington event, on the basis of the uncovered contemporary observational reports around the Eurasian continent, and compare them with the magnetic observations at the time.

The survey on the spatial evolution of the auroral oval benefits a comparison of the intensity of the extreme space weather events, due to the empirical correlation between equatorward boundary of auroral oval and storm intensity in *Dst* index (Yokoyama et al., 1998). While the Carrington event is certainly a benchmark, extreme space weather events such as those in 1872, 1909, and 1921 have been suggested as comparable in terms of the equatorward boundary of auroral visibility (Chapman, 1957a; Hapgood, 2019; Silverman, 2006, 2008; Silverman & Cliver, 2001). Estimating the equatorward boundary of the auroral ovals for these storms supports a feasible comparison of the Carrington event with other extreme space weather events.

Therefore, we first review the evolution of the source active region (AR) on the solar disk at the time. Note that throughout this report, we use the terms “sunspot group” and “active region” as synonyms. We also recover and examine the contemporary auroral reports in the Russian and Japanese archival material, revise the temporal and spatial evolutions of the auroral visibility using known auroral reports (Farrona et al., 2011; Green & Boardsen, 2006; González-Esparza & Cuevas-Cardona, 2018; Hayakawa et al., 2016, Hayakawa, Ebihara, Hand, et al., 2018; Humble, 2006; Kimball, 1960; Moreno Cárdenas et al., 2016), and compare them with available magnetograms (Kumar et al., 2016; Nevanlinna, 2006, 2008). With this

combined information, we contextualize the results in conjunction with those of the other extreme magnetic storms in observational history (see Chapman, 1957a).

2. Method

In this article, we review the contemporary observations of the solar surface and reconstruct the time series of auroral visibility during the stormy interval around the Carrington event. For the observations of the solar surface, we consulted the observational logs by Carrington (1863) and his unpublished manuscripts (RAS MS Carrington 1.3 and 3.2), Schwabe's unpublished observational logs (RAS MS Schwabe 31), and Secchi's reports of his solar observations (OAR MS B13; Secchi, 1859, 1860).

For the auroral visibility, we consulted the observational reports in the yearbook of the Russian Central Observatory (Kupffer, 1860) and the Armagh Observatory (MS 117; see Butler & Hoskin, 1987), newspapers in Portugal, Spain, Australia, New Zealand, and Brazil, and further Japanese diaries and Mexican newspapers (see supporting information Texts S2.1–S2.5). We then compare them with the known records reviewed in Hayakawa, Ebihara, Hand, et al. (2018): reports in contemporary scientific journals (*American Journal of Science* and *Wochenschrift für Astronomie, Meteorologie und Geographie*; see Heis, 1859, 1860), ship logs (see Green et al., 2006; Green & Boardsen, 2006), Australian records (see Humble, 2006; Neumeyer, 1864), newspapers in Spain and Mexico (see Farrona et al., 2011; González-Esparza & Cuevas-Cardona, 2018), Scandinavian reports (see Rubenson, 1879, 1882; Trombolt, 1902) and East Asian historical documents (see Hayakawa et al., 2016, Hayakawa, Ebihara, Hand, et al., 2018). We compute MLAT of the observing sites in the reports, based on the archaeomagnetic field model GUFM1 model covering the position of magnetic dipoles from 1590 to 2000 (Jackson et al., 2000). Note that the canonical archaeomagnetic field model International Geomagnetic Reference Field 12 covers the transition of MLATs only after 1900.

We compare recovered records around the Eurasian continent with the known auroral reports, with magnetic disturbances recorded in the magnetometer at Colaba in Bombay (Kumar et al., 2016), and those in the Russian Empire at that time (Nevanlinna, 2006, 2008) and also update Figures 3 and 4 of Hayakawa, Ebihara, Hand, et al. (2018).

3. The Solar Surface

The storms around the Carrington event occur almost in the maximum of Solar Cycle 10. Figure 1 shows the monthly mean value of the total sunspot number (SSN;Clette et al., 2014 ; Clette & Lefèvre, 2016), with two peaks in October 1859 (SSN: 218) and July 1860 (SSN: 222). Likewise, the monthly mean value of the smoothed sunspot area (Carrasco et al., 2016) shows two peaks in September 1859 (2,300 millionth of solar hemisphere = msh) and July 1860 (2,270 msh). Frequently, the SSN has two peaks for each cycle, mostly due to the two separated activity maxima of the northern and southern hemispheres (Gnevyshev, 1963; Storini et al., 2003). We contextualize the 1859 storms slightly before the first peak in the SSN and exactly at the first peak in the smoothed sunspot area.

During this enhanced phase near the first peak in Solar Cycle 10, a significantly large and complex sunspot group appeared on the solar disk, which was visible even without a telescope (Crookers, 1859, p. 68; cf. Vaquero & Vázquez, 2009, pp. 57–102; Hayakawa et al., 2017, Hayakawa, Willis, et al., 2019). This large sunspot group was monitored by a number of contemporary astronomers such as Secchi, Carrington, and Schwabe. Among them, Father Angelo Secchi was the director of Collegio Romano and a prominent scientist and sunspot observer at that time. He mentioned this group's association with the great auroral display: “It is extremely remarkable that these great perturbations should have coincided with a maximum of solar spots, and should have happened precisely at a moment when an immense spot was visible on the disc of the Sun, even without the aid of the telescope” (Crookers, 1859, p. 68).

Within this large sunspot group, Carrington (1859) and Hodgson (1859) witnessed the earliest white-light flare in observational history on 1 September. This flare was recorded at 11:18–11:23 UT on 1 September and followed by a synchronized magnetic crochet ≈110 nT in the horizontal force at the Earth (Carrington, 1859; Cliver & Svalgaard, 2004; Hodgson, 1859; Stewart, 1861). Note that the source flare for

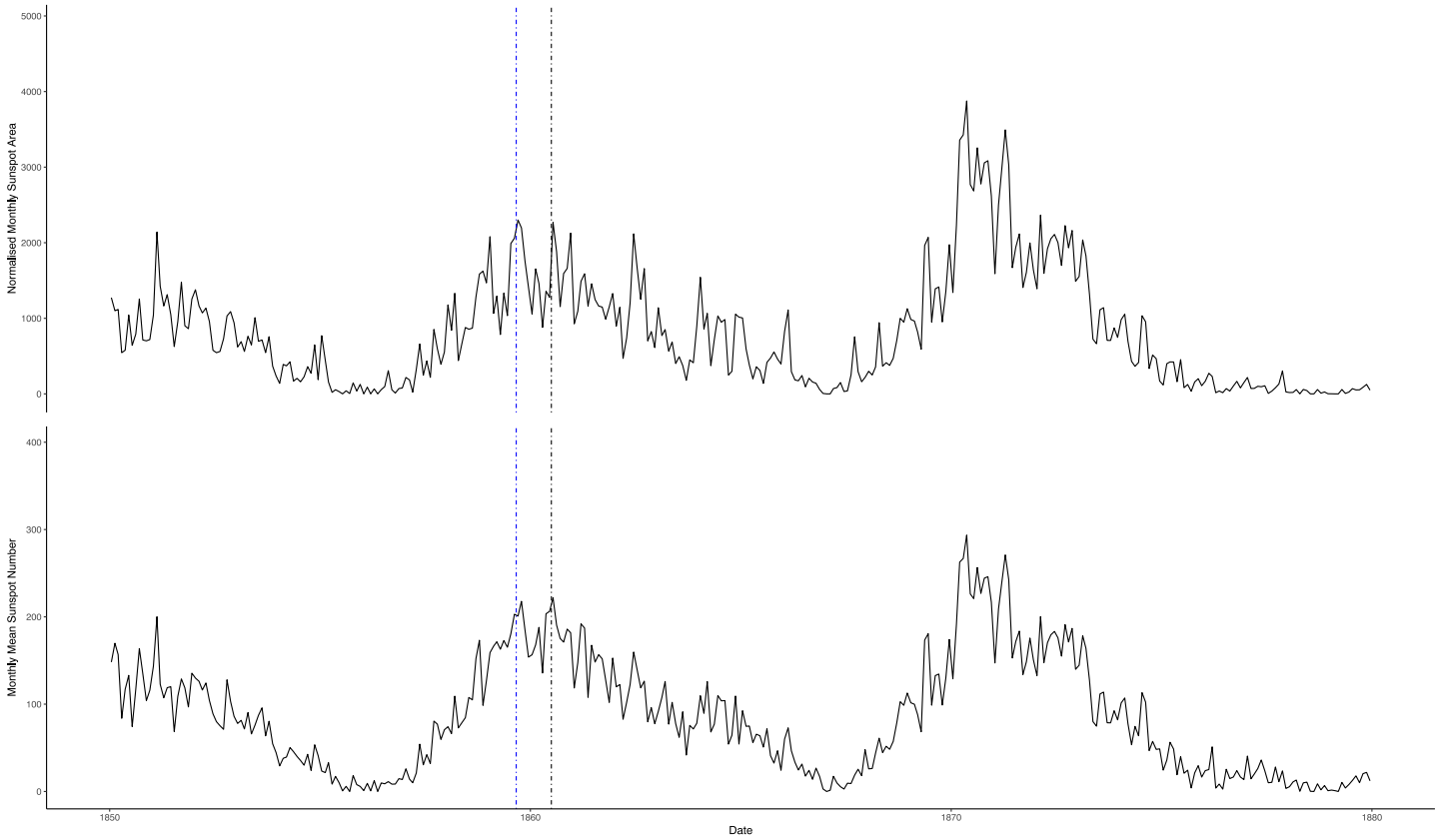

Figure 1. The extreme storms around the Carrington event in 1859 (gray bar) in comparison with the double peak of the monthly mean value of the total sunspot number provided from Sunspot Index and Long-term Solar Observations (Clette et al., 2014; Clette & Lefèvre, 2016) in the lower panel and the monthly mean value of the smoothed sunspot area (Carrasco et al., 2016) in the upper panel.

the August storm had not been captured by other contemporary observers so far (e.g., Neidig & Cliver, 1983; Vaquero et al., 2017). This is not surprising, as the time span of the flare itself in white light is not long and contemporary observers had no concept of a flare watch before this discovery.

The exact position and morphology of the sunspot group responsible for these events can be reconstructed from the sunspot drawings and associated observational logs by contemporary observers. In particular, the sunspot group associated with the Carrington flare was recorded not only in Carrington's sunspot drawings but in those by Schwabe and Father Secchi as well. Figure 2 shows Carrington's drawings of a whole solar disk and of the sunspot group that generated an intense flare on 1 September. Figure 3 shows Schwabe's sunspot drawings on 27 August and 1 September 1859. Figure 4 displays Father Secchi's solar observations on 28 and 31 August 1859.

Comparison between Figures 2 and 3 shows different viewing aspects in Carrington drawing than in the whole Sun drawing by Schwabe. Carrington used a 4.5-in. (11.43 cm) refractor, which had a focal length of 52 in. (1.32 m), with an equatorial mount and applied a projection method to obtain the solar disk with a diameter of 11 in. (27.94 cm) for his sunspot observations (Carrington, 1863; Cliver & Keer, 2012). Because of a projected image on a screen, the Sun's north and west are found in the upper and left sides of his original sunspot drawing, respectively. On the other hand, Schwabe used two Keplerian telescopes in which one had a reduced aperture of 1.75 in. (4.45 cm) and a focal length of 3.5 ft (1.07 m) and the other had a reduced aperture of 2.5 in. (6.35 cm) and a focal length of 6 ft (1.83 m) and dimming glasses to observe sunspots with a direct viewing method (Arlt, 2011; Johnson, 1857). Therefore, his sunspot drawings show a solar image that is reversed in the north-south and east-west directions. The orientation of Schwabe's drawing is in the celestial coordinate system with north pointing down (Arlt et al., 2013).

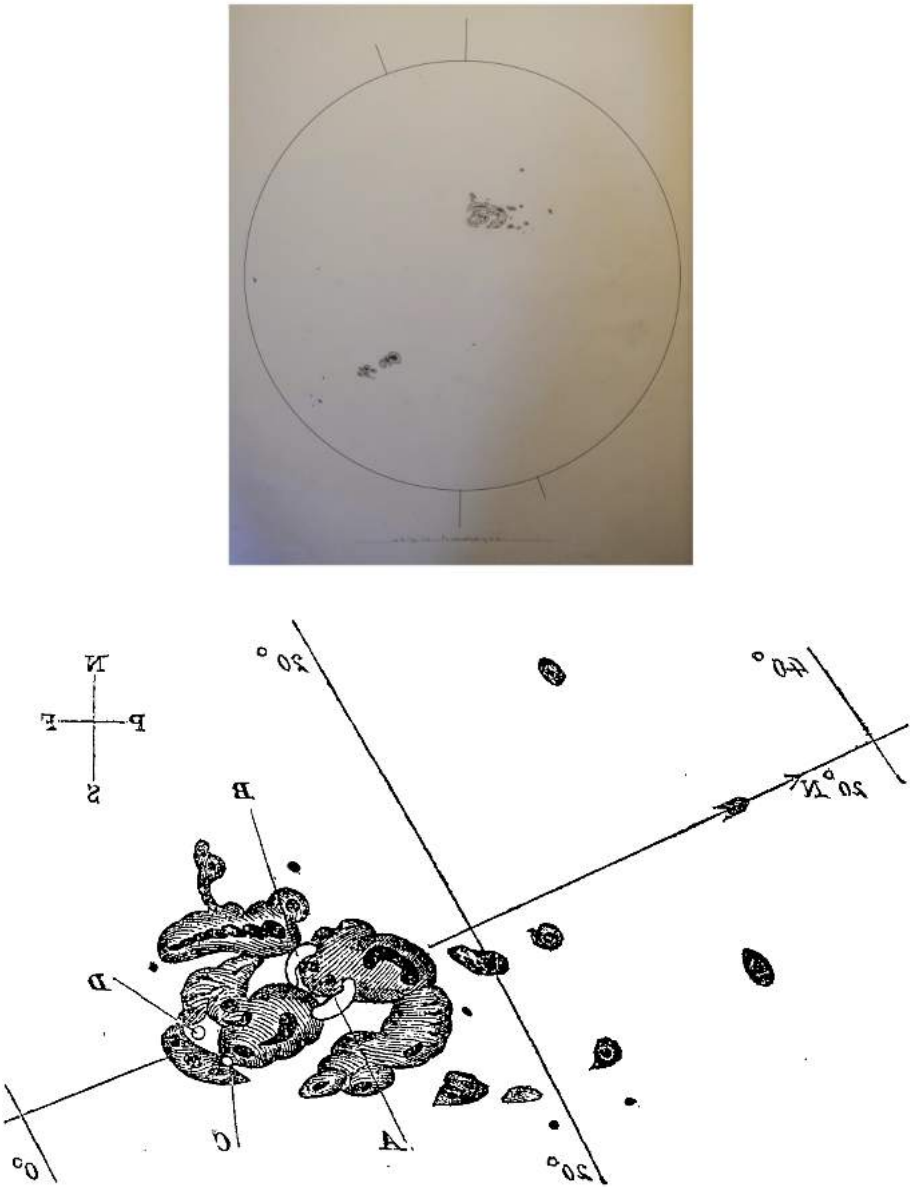

Figure 2. Drawings of a whole solar disk (top) and of the sunspot generated the strongest white-light flares (bottom) made by Richard Carrington on 1 September with its limb enhanced (RAS MS Carrington 3.2, f. 313a; Image courtesy of the Royal Astronomical Society). In both of panels, drawings are reversed from the originals in the horizontal direction as seen in the original solar disk. In the top panel, the Sun's rotational axis is drawn as an oblique line, and the sunspot that caused the Carrington flare is in the upper-right quadrant of solar disk.

Secchi's observations were conducted with a Cauchoix achromatic telescope, which had an aperture of 16.9 cm and a focal length of 238 cm, with projection of solar image of diameter equal to 246 mm (Secchi, 1859; OAR MS B13; see also Altamore et al., 1921). In order to make the comparison feasible, we recast the original solar disk drawings in Figures 2–4, as seen in the sky, on the basis of each observational method. Comparison between Figures 2, 3, and 4 shows that the locations of sunspots in the Schwabe and Secchi's whole disk drawings are consistent with those in Carrington's drawings.

The sunspot group associated with the Carrington flare is Group 520 in Carrington (1863, p. 167), whereas Schwabe (RAS MS Schwabe 31; Figure 3) separated this group to Groups 143 and 142. Note that Schwabe's close-up drawing of Group 143 and Carrington's drawing of Group 520 have been reversed in Figures 2 (Carrington) and 3 (Schwabe). Thus, Schwabe's drawing resembles Carrington's drawing in a general view of the sunspot group. The entire sunspot group may be identified as an Fki-type group in the McIntosh

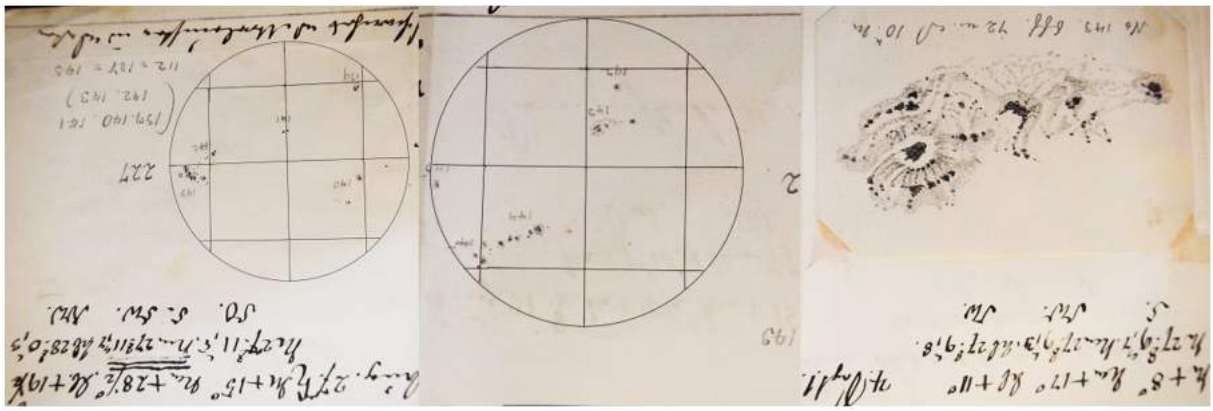

Figure 3. Sunspot drawings by Heinrich Schwabe on 27 August (left), 1 September (center), and close-up figure of 1 September (right), reproduced from RAS MS Schwabe 31 (p. 131 and p. 136; Image courtesy of the Royal Astronomical Society). Circles in the upper halves correspond to the solar disk, on which the sunspots are drawn with the numbers. The sunspot group that caused the Carrington flare is numbered 143 (on left side of the disk in the left panel and a little upper right of the disk center in the middle panel). Note that Schwabe separated Carrington's Group 520 to Groups 143 and 142. Close-up drawing in the right panel reveals the details of the Group 143. They are reversed as they were seen on the sky. The solar rotational axis is not shown in these drawings. Their limb and contrast have been enhanced here.

(1990) classification, but the depictions of umbrae are different from each other. This sunspot group is also captured in heliograms acquired at the Kew Observatory (RGO 67/266; Figure 5 of Cliver & Keer, 2012) and Secchi's projected sunspot drawings (Group 219 with a smaller Group 218 in Figure 4). The sunspot groups recorded in these sources show significantly similar sunspot morphology to those in Carrington's sunspot drawings. Therefore, it is conceivable that the differences in the depiction of umbrae between Carrington and Schwabe stem from difference of their observational methodologies.

These sunspot drawings and heliograms show significantly complex topology of this source AR and indicate strongly mixed magnetic polarity. In theory, the white-light brightenings, which are the foot points of strong electron beaming from the reconnection site, should be located on both sides of the polarity inversion line. If this is the case, the polarity inversion line crosses the middle of this spot group, indicating a delta configuration, the most flare-productive category of the sunspots (see Toriumi et al., 2017; Toriumi & Wang, 2019; Zirin & Liggett, 1987).

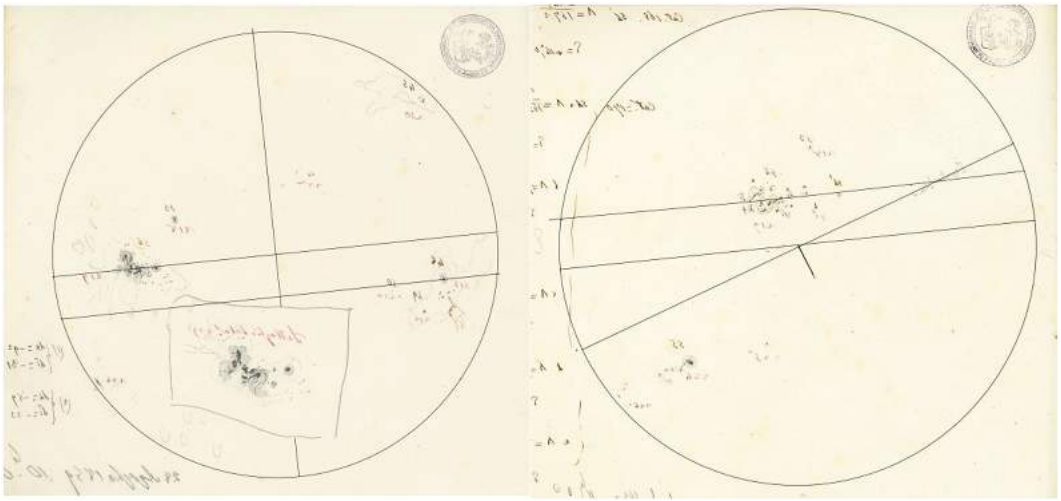

Figure 4. Drawings of the solar disk by Father Angelo Secchi on 28 (left) and 31 (right) August 1859 (OAR MS B13 in Archivio INAF Osservatorio Astronomico di Roma). The left observation includes close-up drawing of the source region of the Carrington event. In both of panels, drawings are reversed from the originals in the horizontal direction as seen in the original solar disk. The solar rotational axis is shown as a short oblique line in the right drawing. Their limb and contrast have been enhanced here.

Schwabe associated the Group 143 with other sunspot groups in early August (127) and early July (112). If this is indeed the case, this group had been extant and recurrent at least for three solar rotations, as is frequently the case with large sunspot groups (Henwood et al., 2010; Namekata et al., 2019). Interestingly, the aurora was reported in China on 4 August 1859 (see Willis et al., 2007), and a negative excursion was recorded in Russia in late September (see Veselovsky et al., 2009), which may support the recurrence of this large sunspot group. Further surveys are required to document the entire lifespan of this AR.

The original sunspot drawings show that this sunspot group appeared in the eastern limb on 25 August 1859, came across the central meridian around 31 August and 1 September 1859, and went beyond the western limb by 7 September 1859 (Arlt et al., 2013; Carrington, 1863). On 1 September, the sunspot was situated at N27.5°–N12.4° in latitude, W28.7°–W6.6° in longitude at ≈11.2 hr UT (Carrington, 1863, p. 83) and N20.5°–N16.8° in latitude, W24.3°–W8.8° in longitude at ≈9.2 hr UT (RAS MS Schwabe 31; Arlt et al., 2013), being geoeffectively favorable (e.g., Gopalswamy et al., 2005, 2012; Schrijver et al., 2012).

The Carrington flare on 1 September was probably preceded by a flare event associated with the August storm. While its onset is not recorded, we may expect it to have occurred somewhere around 27 August, assuming a coronal mass ejection (CME) transit time of ≥1 day (e.g., Gopalswamy et al., 2005; Lefèvre et al., 2016). The disk center was mostly without sunspots, except for a tiny group (141), situated at N20.9°–N20.7° in latitude, W6.0°–W3.3° in longitude (RAS MS Schwabe 31; Arlt et al., 2013). The only large group (143), which was separated from a small group (142), was situated far eastward then, roughly at E57°, N13° at ≈9.2 hr UT (RAS MS Schwabe 31; Arlt et al., 2013). It is quite notable that this sunspot group seemingly managed to cause a geoeffective interplanetary CME (ICME) even with this unfavorable location (cf. Gopalswamy et al., 2005 ; Lefèvre et al., 2016). Cliver (2006) considered the ICME hit the Earth "only a glancing below" and was probably even larger than that of the September storm, assuming the calculated longitude of E55°–E60°.

Subsequently, another great aurora was reported even down to Athens (Heis, 1861, p. 115; N37°58′, E23°44′, 37.2° MLAT) with a simultaneous extreme magnetic disturbance seen on the Bombay magnetogram ($\Delta H \approx 984$ nT) on 12 October 1859 (see Kumar et al., 2016; Lakhina & Tsurutani, 2017), while the latter seems associated with another sunspot group.

4. Auroral Evolutions and Magnetic Disturbances

The large sunspot group (Group 520 in Carrington, Group 143 in Schwabe, and Group 219 in Secchi) caused a series of ICMEs, and a subsequent series of magnetic storms and auroral displays between 28 August and 4 September 1859 (Green & Boardsen, 2006; Hayakawa, Ebihara, Hand, et al., 2018; Kimball, 1960; Lakhina et al., 2013; Lakhina & Tsurutani, 2017).

Table S1 in the supporting information shows the visual auroral reports around the Eurasian continent during this time interval, recovered in this article. The Russian yearbook reports auroral displays on 28/29 August at St. Pétersbourg (56.9° MLAT) and Sitka (59.3° MLAT). The September auroral displays in Russia were seen more widely on 1/2–4/5 September, throughout the Siberian stations down to Nertschinsk (40.0° MLAT) and Barnaoul (43.2° MLAT). Japanese diaries enable us to add five more auroral reports on 1/2 September that show moderate auroral visibility on the northern coast of Japan. The aurorae were visible down to Hakata (22.6° MLAT), slightly more equatorward than previously known (23.1° MLAT; Hayakawa et al., 2016).

From western Europe, auroral records have been recovered in the meteorological records (MS 117) in the Armagh Observatory (see Butler & Hoskin, 1987) and Portuguese and Spanish newspapers. The Armagh records show relatively long auroral visibility during the nights of 28 and 29 August and 2–4 September. The Portuguese and Spanish newspapers show intensive auroral displays on 28 August, which extended even beyond the zenith at Portuguese cities and formed corona aurorae at Lisbon (Pt1: 44.3° MLAT).

From Oceania, we found a series of newspapers in New Zealand and Western Australia. The newspapers in New Zealand reported aurorae mostly on 29 August, whereas those in Western Australia reported them on 2 September. We also surveyed Mexican and Brazilian newspapers. Consequently, we located two more auroral reports in Mexico. We found no newspapers mentioning auroral observations in Brazil in the database of the National Digital Library of Brazil (http://bndigital.bn.gov.br), while two Brazilian newspapers

mentioned auroral visibility at Lisbon (O Cearense, 11 November 1859) and Montreal and New England (Correio da Tarde, 10 December 1859).

We have integrated these recovered auroral reports from Russian, Irish, Portuguese, Oceanian, Mexican, and Japanese documents with the previously known *datable* auroral reports (see e.g., Green & Boardsen, 2006; Hayakawa, Ebihara, Hand, et al., 2018; Kimball, 1960). Note that the Russian Empire ruled Alaska at that time and had preserved a report at Sitka in Alaska. We have plotted their spatial and temporal extents in Figures 5 and 6. Figure 5 shows the spatial extent of the auroral visibilities on 28/29–29/30 August and 1/2–2/3 September 1859 on the basis of visual auroral reports from known data sets and new archival records around the Eurasian continent. This figure shows explicitly that the new data fill the existing gap of observations around the Eurasian continent, especially in the Eastern Hemisphere (e.g., Green & Boardsen, 2006; Kimball, 1960). These auroral observational sites are partially overlapping with the locations of magnetograms in Russia (Nevanlinna, 2008).

Figure 6 shows the temporal extent of the auroral visibility during the stormy interval between 28/29 August and 4/5 September 1859. The auroral displays were intermittently visible from 28/29 August to 4/5 September, with two remarkable bands on 28/29 August down to ≈20.2° MLAT and 1/2–2/3 September down to ≈20.5°/21.8° MLAT. This figure shows the data with a explicit description on start and end of auroral visibility. There are additional reports (not shown) with auroral visibility between these two bands, without a clear description of their start and end. Therefore, some observational records in this interval such as those at Armagh are not plotted in this figure, as they do not have explicit description for the start and end of their visibility.

The onset of the first cluster of storms is confirmed as a sudden commencement at 21 hr UT on 28 August (Jones, 1955, p. 104). The onset of the auroral visibility is reported roughly after 20.5 hr UT on 28 August. This is probably because the auroral oval extended more actively in western Europe and North America and started to be visible after dark there.

The second outburst of auroral displays is almost synchronized with the onset of the sharp negative excursion at Bombay around 4.3–6.7 hr UT on 2 September (see also Hayakawa, Ebihara, and Hand et al., 2018). Because this negative excursion falls in the daytime in the Eastern Hemisphere (9.2–11.6 hr local mean time, LMT, at Bombay), the auroral displays were mainly reported not in the Eastern Hemisphere but in the Western Hemisphere, such as in the cities along the Caribbean Coast (down to ≈22.8° MLAT) and Chile (≈−21.8° MLAT), with the equatorward boundary of auroral oval around ≈30.8° ILAT.

Indeed, aurorae were visible in most equatorward stations immediately after the magnetic negative excursion (4.3–6.7 hr UT). The auroral visibility at Sabine (RG24-2: N11°32′, W083°49′, 23.1° MLAT), St. Mary's (RG24-3: N12°30′, W088°25′, 23.0° MLAT), at a ship in the Atlantic Ocean (WA1: N14°28′, W024°20′, 22.8° MLAT), and Santiago (S33°28′, W070°40′, −22.1° MLAT) were reported from 6.1, 5.9, 6.1, and 6.2 hr UT, respectively (see Table 1 of Hayakawa, Ebihara, Hand, et al., 2018). Moreover, if we date the report at Honolulu (20.5° MLAT in visibility and 28.5° ILAT in magnetic footprint) on 1/2 September as in Kimball (1960), the onset of its auroral visibility is 22 hr on 1 September in LMT and calculated 8.5 hr on 2 September in UT, which is slightly after this negative excursion at Bombay.

This timing may explain why the number of auroral reports from Southern Europe during the August storm is larger than that during the September storm. This negative excursion (4.3–6.7 hr UT) falls almost at the end of night in the European sector. Taking Lisbon (N38°43′, W009°08′), one of the westernmost cities in the European sector and hence with one of the sites with the latest sunrise in this sector, as reference, the duration of this negative excursion (4.3–6.7 hr UT) was probably affected by twilight and even daylight, as the local sunrise and the local onset of astronomical twilight are calculated as 06:06 UT and 04:33 UT. The Portuguese newspaper at Horta (N38°32′, W028°38′, 47.2° MLAT) confirms this hypothesis describing the auroral visibility from 5.9 UT on 2 September (28 LMT on 1 September in Table S1) "until the dawn light dimmed it" (Pt6).

Nevertheless, the auroral displays remained visible through the recovery phase of the storm and enabled observers in the Russian Empire and East Asia (down to ≈22.6° MLAT), and even in Mid-Europe, to see these displays into the next night wherever the actual equatorward boundary of auroral oval was at that time.

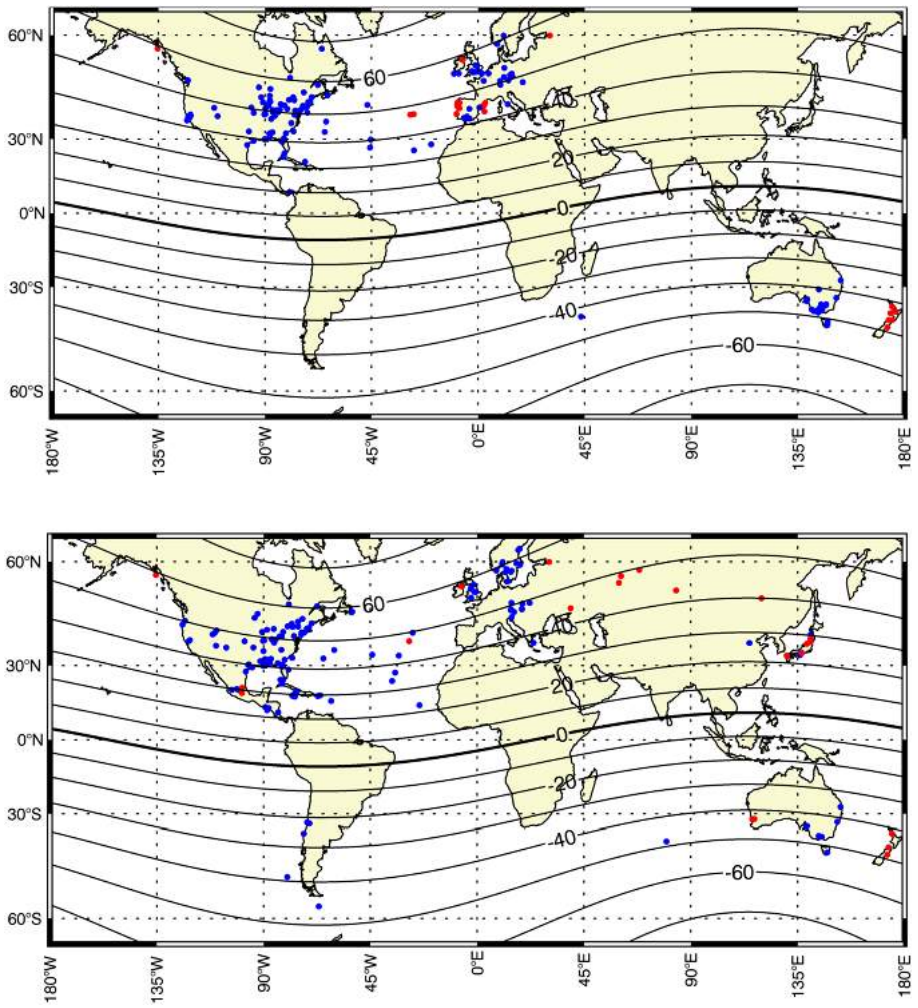

Figure 5. Auroral visibility on 28/29–29/30 August (top panel) and 1/2–2/3 September 1859 (bottom panel) reconstructed from visual auroral reports. The archival records recovered in this article are depicted in red color, whereas the previously known observational sites are depicted in blue color. The observation at Honolulu is not included here due to its dating uncertainty.

The magnetogram at Bombay (N18°56′, E072°50′; 10.3° MLAT, E140.5° magnetic longitude [MLON]; see Figure 4 of Hayakawa, Ebihara, Hand, et al., 2018), whose relative position against the auroral oval was discussed in the context of the possible contribution of ionospheric currents (Cliver & Dietrich, 2013; Green & Boardsen, 2006), is situated in the Eastern Hemisphere and neighbored by the observational sites in the Russian Empire and East Asia (Figure 7). While the visual auroral reports from these sites do not provide records with an elevation angle, we can combine these reports to make conservative estimates for the equatorward extension of the auroral ovals during this stormy interval. The magnetic coordinates of the Siberian station at Nertschinsk (N51°19′, E119°36′) on 2 September are computed as 40.0° MLAT and W175.5° MLON. This station is situated in a similar magnetic longitude to the auroral observational sites in East Asia such as Inami (HJ2, 23.2° MLAT, W160.4° MLON; N33°49′, E135°59′) and Luánchéng (HC1, 26.5° MLAT, W179.6° MLON; N37°54′ E114°39′; see Hayakawa, Ebihara, Hand, et al., 2018).

In order for these aurorae to be visible at Inami up to 10° in elevation angle (see, e.g., Shiokawa et al., 1998), the equatorward boundary of the auroral oval needs to be down to, at least, 37.6° ILAT, assuming an auroral elevation up to 400 km (Ebihara et al., 2017; Silverman, 1998). This means the equatorward boundary of the auroral oval was at least extending beyond the zenith of Nertschinsk (40.0° MLAT) during the period of auroral visibility in China and Japan. According to the record at Inami (HJ2), the aurora started to be visible from ≈16 LT (≈07 UT), which is before sunset. Conservatively, we assume that the aurora actually started to be visible from nautical twilight, that is, ≈10.3 UT on 2 September.

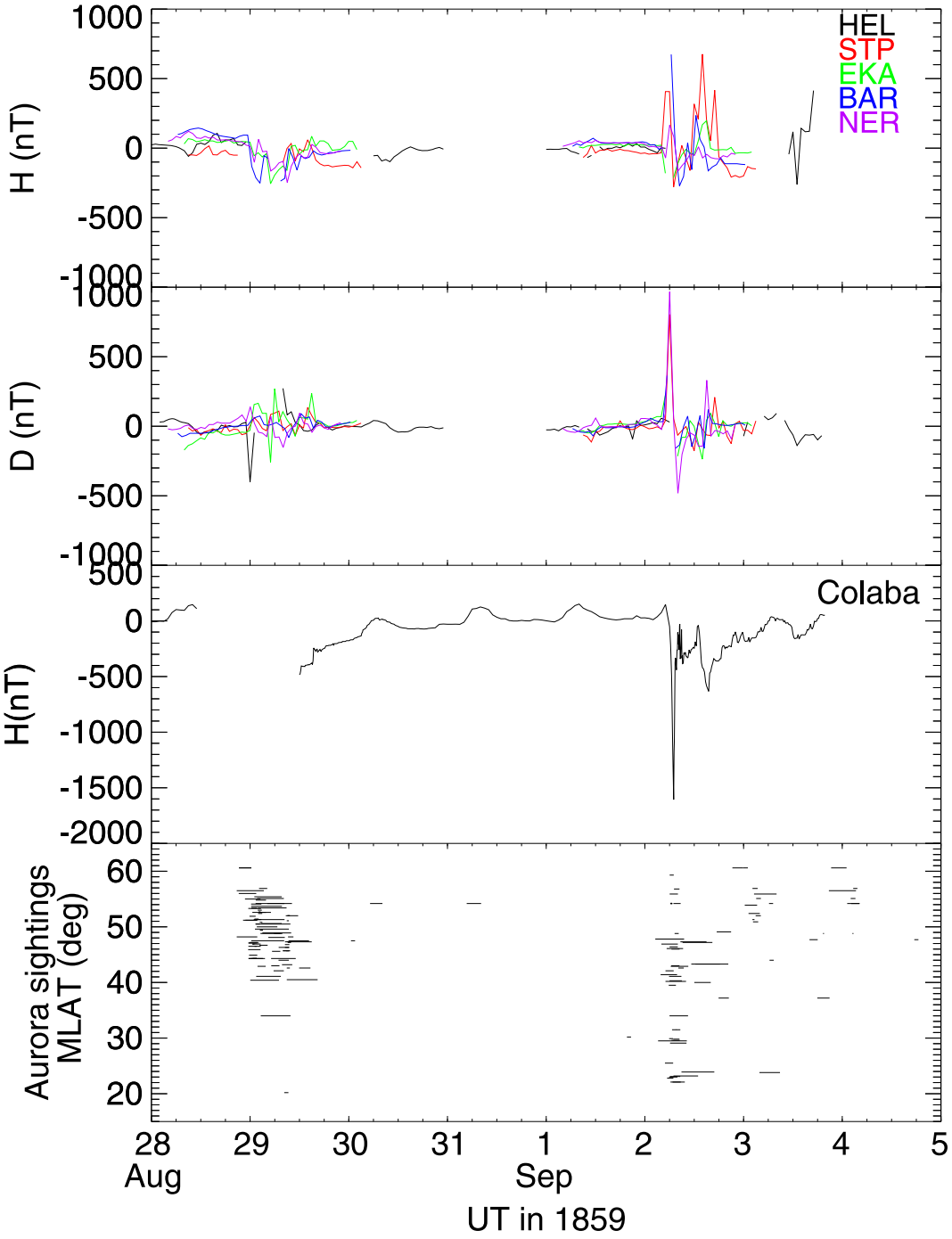

Figure 6. The lower panel is the time series of auroral visibility from 28 August to 5 September with UT on horizontal axis. The corresponding magnetic latitude (MLAT) is on the vertical axis. This time series is compared with the magnetograms in the Russian Empire in the upper panels derived from Nevanlinna (2006, 2008) and that of the Colaba Observatory in the third panel. Data from Colaba is a reproduction of Figure 4 of Hayakawa, Ebihara, Hand, et al. (2018). The abbreviations on the panels for declination (D) and horizontal force (H) in the Russian Empire (the first and second panels) signify observational sites: HEL (Helsinki), STP (St. Pétersbourg), EKA (Catherinbourg), BAR (Barnaoul), and NER (Nertschinsk).

As shown in Figures 6 and 7, a positive excursion of the H-component magnetic field at Nertschinsk had ended by the time the aurora started to be visible at Inami. Since Nertschinsk was located in the noon-dusk sector, this positive excursion is probably due to the eastward Hall current flowing in the ionosphere, which is a part of the DP2 current system (Nishida, 1968). It is plausible that the enhancement of the DP2 current

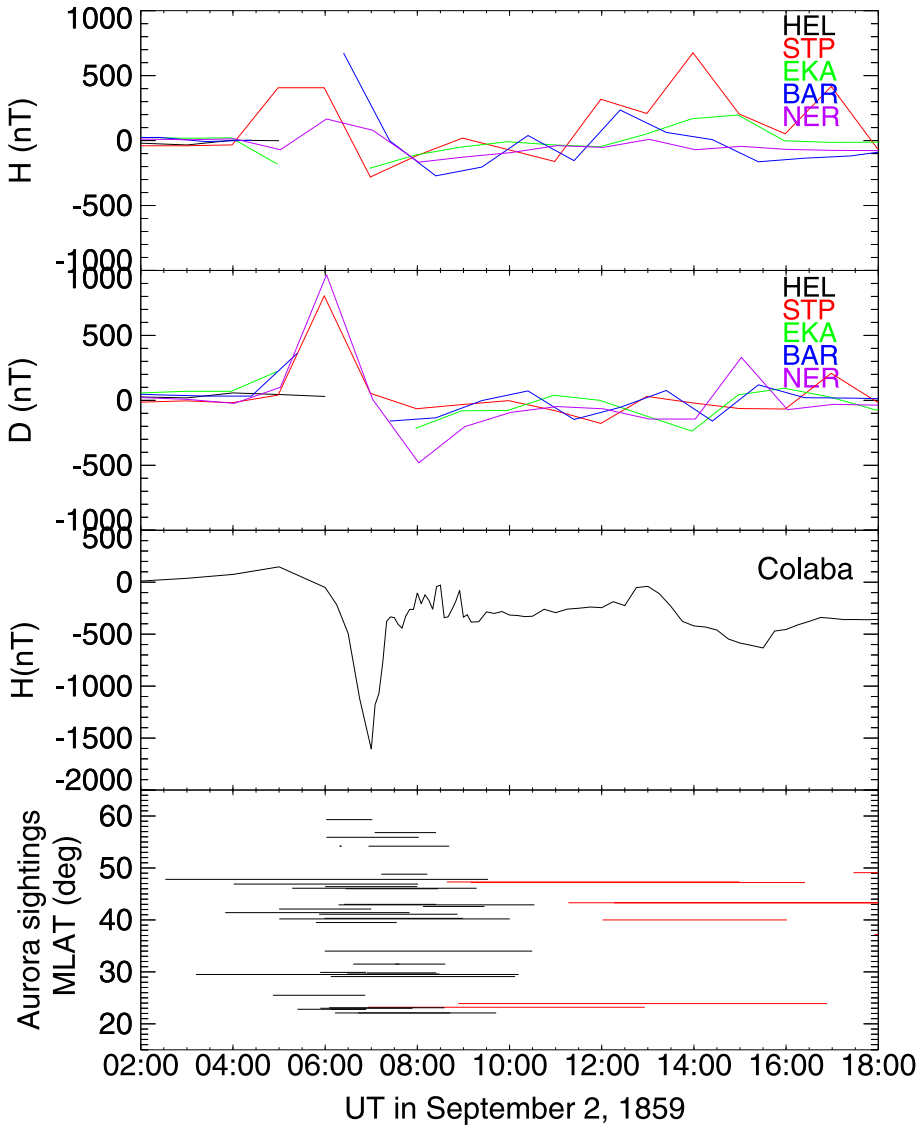

Figure 7. Close-up view of part of Figure 6. The horizontal red lines in the bottom panel indicate the auroral visibility at E072°50′ ± 90° geographic longitude (i.e., in the longitudinal sector centered on Bombay). Data from Colaba is a reproduction of Figure 4 of Hayakawa, Ebihara, Hand, et al. (2018).

system, namely, the convection, had just ended by this moment. If so, the enhancement of the convection could have transported cold or warm electrons (Ebihara et al., 2017) deep into the inner magnetosphere to become seed electrons of the aurora. The electrons transported earthward by the convection would remain for a while after the weakening of the convection. The remnant of the electrons is thought to result in the aurora that was visible at HJ8 until ~17 UT on 2 September. The bipolar variations of the D-component of the magnetic field at Nertschinsk and St. Pétersbourg (≈05–10 UT) are difficult to understand and will be studied further in the future.

5. Comparison of the Spatial Evolution of the Auroral Ovals for Extreme Events

Having presented an updated view of the spatial evolution of the auroral ovals during the stormy interval around the Carrington event, we can categorize the Carrington event not as an exceptionally outstanding event but as one of the most extreme events by comparison with the spatial evolution of the auroral oval for other extreme magnetic storms. Note that the spatial extent of the equatorward boundary of the

auroral oval has a good empirical correlation with the storm intensity as indicated by the *Dst* index (Yokoyama et al., 1998).

During the stormy interval around the Carrington event, the absolute value of the auroral visibility was reported down to ≈20.2° MLAT on 28/29 August and ≈20.5° MLAT or ≈21.8° MLAT on 1/2 September. In concert, the equatorward boundary of auroral oval was reconstructed as ≈36.5° ILAT on 28/29 August and ≈28.5° ILAT or ≈30.8° ILAT on 1/2 September (see also Hayakawa, Ebihara, Hand, et al., 2018).

The *Dst* value of the Carrington event is still under discussion (e.g., Cliver & Dietrich, 2013; Gonzalez et al., 2011; Siscoe et al., 2006; Tsurutani et al., 2003). Here we need to note that, by definition, the *Dst* value is reconstructed from hourly averages of the horizontal force at four midlatitude stations. (e.g., Sugiura, 1964; Sugiura & Kamei, 1991). In this sense, the estimates of *Dst* ≈ −900 (+50, −150) nT on the basis of hourly average of the horizontal force at Bombay better probably better the *Dst* value, although this is a single station measurement and hence we still need three more stations for a more standard representation (Cliver & Dietrich, 2013; Gonzalez et al., 2011; Siscoe et al., 2006).

These values are contextualized by comparison with other extreme storms with "outstanding auroras" in February 1872, September 1909, and May 1921 (see Chapman, 1957a). The equatorward boundary of the auroral oval for the extreme storm on 4 February 1872 is reconstructed as ≈24.2° ILAT, based on the reports of overhead aurora up to the zenith at Shanghai (19.9° MLAT) and Jacobabad (19.9° MLAT; e.g., Chapman, 1957b; Hayakawa, Ebihara, Willis, et al., 2018). The auroral displays themselves are reported down to Shàoxīng (18.7° MLAT; Hayakawa, Ebihara, Willis, et al., 2018) and arguably down to Bombay (10.0° MLAT; Chapman, 1957a; Silverman, 2008). The magnetogram at Bombay showed the *Dst* value to be probably <−830 nT, on the basis of a preliminary value from a single station.

Likewise, regarding the extreme magnetic storm on 25 September 1909, the equatorward boundary of the auroral oval is reconstructed as 31.6° ILAT, on the basis of the report from Matsuyama (23.1° MLAT) with an elevation angle of 30° (Hayakawa, Ebihara, et al., 2019). The aurora was also reported from Singapore (−10.0° MLAT), although Silverman (1995) casts doubt on its reliability due to possible contamination from reports of telegraph disturbance. Its *Dst* value was reconstructed as −595 nT, based on the magnetic observations at Apia, Mauritius, San Fernando, and Vieques (Love et al., 2019a).

Regarding the extreme magnetic storm on 14/15 May 1921 (Hapgood, 2019; Silverman & Cliver, 2001), the aurora was reported down to Apia with a significant magnetic disturbance (Angenheister & Westland, 2005, p. 202). The *Dst* value is computed to be ≈−907 ± 132 nT, on the basis of magnetograms at Apia, Vassouras, San Fernando, and Watheroo (Love et al., 2019b). The MLAT of Apia is computed as −16.2° MLAT based on the authorized International Geomagnetic Reference Field dipole model (see Thébault et al., 2015). The auroral display was "reaching to an altitude of 22° determined from star positions noted" (Angenheister & Westland, 2005, p. 202). Accordingly, we reconstruct the equatorward boundary of the auroral oval as 27.1° ILAT.

These values are comparable to those of the Hydro-Quebec event on 13/14 March 1989, with the most extreme *Dst* value within the coverage of the official *Dst* data set (WDC for Geomagnetism Kyoto, 2015). During this storm, the aurora was visible down to 29° MLAT (Silverman, 2006), and auroral particle precipitation and the auroral electric field were confirmed down to ≈40.1° MLAT and ≈35° MLAT in the satellite imagery (Rich & Denig, 1992), although that relationship with the visual auroral oval is not completely clear.

As shown in Table 1, the spatial extent of the Carrington event is comparable to that of other outstanding auroras. As far as currently known, the spatial extent of the equatorward boundary of the auroral oval is most extreme in the February 1872 event (≈24.2° ILAT), immediately followed by that of the May 1921 event (≈27.1° ILAT) and then the Carrington event (≈28.5°/30.8° ILAT), while the spatial extent of the Carrington event varies depending on the dating uncertainty in the report from Honolulu (see Hayakawa, Ebihara, Hand, et al., 2018).

Given the empirical correlation between the equatorward boundary of the auroral oval and the storm intensity in *Dst* value (Yokoyama et al., 1998), it seems that the *Dst* value of the Carrington event (September storm) is more likely to be ≈−900 (+50, −150) nT as an hourly average (Cliver &

Table 1
Comparison of the EB of the Auroral Oval in Absolute Value and the Dst Values of the Outstanding Auroras With the Hydro-Quebec Event on 13/14 March 1989, Based on RD92 (Rich & Denig, 1992), S+06 (Siscoe et al., 2006), H+18a (Hayakawa, Ebihara, Willis, et al., 2018), H+18b (Hayakawa, Ebihara, Hand, et al., 2018), H+19a (Hayakawa, Ebihara, et al., 2019), L+19a (Love et al., 2019a), and L+19b (Love et al., 2019b)

Event			EB of visibility (MLAT)	EB of oval (ILAT)	*Dst* value (nT)	Reference
Year	Month	Date				
1859	8	28/29	20.2	36.5	≥−484[a]	H+18b
1859	9	1/2	20.5/21.8	28.5/30.8	≈−900 (+50, −150)[a]	S+06 and H+18b
1872	2	4	10.0/18.7	24.2	<−830[a]	H+18a
1909	9	25	10.0/23.1	31.6	−595	H+19a and L+19a
1921	5	14/15	16.2	27.1	−907 ± 132	This work and L+19b
1989	3	13/14	29	35/40.1	−589	RD92

Note. The equatorward boundary of the auroral oval for the Hydro-Quebec Event is based on auroral particle precipitation and the auroral electric field. MLAT = magnetic latitude; ILAT = invariant latitude; EB = equatorward boundary.
[a]A preliminary value using single-station data in hourly average, due to the limited availability of complete magnetogram in middle to low latitude (see, e.g., Hayakawa, Ebihara, et al., 2019; Love et al., 2019a). The Dst values are shown in the hourly value or its equivalence, whereas the data in higher time resolution tends to show larger values than the hourly values such as those for the 1859 event (−1760 nT; Tsurutani et al., 2003) and the 1989 event (−720 nT: Gannon & Love, 2011).

Dietrich, 2013; Siscoe et al., 2006), whereas the maximal amplitude of horizontal force at Bombay was reported 1760 nT (Tsurutani et al., 2003). This hourly value is comparable to that of the May 1921 storm (see Love et al., 2019b). This comparison tells us that the Carrington event was not likely unique but one of the most extreme events.

Regarding the August 1859 storm, the minimum ΔH is conservatively estimated to be ⍰−484 nT, as the Colaba magnetogram failed to record its main phase on Sunday (Hayakawa, Ebihara, Hand, et al., 2018). Colaba was situated on the evening side where the contribution from the ring current is large (Cahill, 1966). Therefore, it is conservatively speculated that minimum *Dst* was comparable to or slightly larger than −484 nT.

While the current space weather community expects this kind of event to happen once a century with a potential catastrophe for the modern society (Baker et al., 2008; Daglis, 2001; Dyer et al., 2018; Hapgood, 2011; Riley, 2012; Riley et al., 2018; Riley & Love, 2017; Schrijver et al., 2012), the historical evidence indicates that we need to be slightly more careful about the meaning of "extreme space weather events." We were quite fortunate that the extreme ICME in July 2012 missed the Earth. Some estimates of its potential *Dst* value appear to be even more extreme than that of the Carrington event (Baker et al., 2013; Liu et al., 2014, 2019; Ngwira et al., 2013). The extremely fast ICME on 4 August 1972 hits the Earth with its interplanetary magnetic field dominantly northward (Knipp et al., 2018; Tsurutani et al., 2003), causing short-term and local magnetic enhancements that do not appear as part of the *Dst* record. This storm was very geoeffective even in the absence of a deeply negative *Dst* value (Knipp et al., 2018). These episodes in the history of space weather indicate that the Carrington event is certainly one of the most extreme events but is not the single exceptional extreme event.

6. Conclusion

In this article, we have revised the temporal and spatial evolutions of the auroral displays during the stormy interval around the Carrington event. The contemporary sunspot drawings by Richard Carrington, Heinrich Schwabe, and Father Angelo Secchi showed a large and complex source AR between 25 August and 7 September. Schwabe and Secchi's sunspot drawings let us confirm the sunspot topology detailed in Carrington's (1859) sunspot drawings (Hayakawa, Ebihara, Hand, et al., 2018) with their resemblance, even though Schwabe's methodology is different from Carrington's for the solar observation. This resemblance is important because the scientific discussions of the Carrington event have been based on Carrington's drawing, and now they are strengthened by these additional contemporary observations. This AR probably caused a significant ICME on 27 August resulting in the first magnetic storm on 28/29 August, despite the AR's unfavorable location on the eastern side of the solar disk. The source AR rotated to the disk center on 31 August to 1 September and caused the white-light flare on 1 September, associated with the second extreme magnetic storm with low latitude aurorae.

The visual auroral reports from the Russian Empire and Japan enable us to fill the apparent gap of auroral observations in the Eastern Hemisphere and complimentarily show a long and intermittent auroral visibility through the stormy period from 28/29 August to 4/5 September, when compared with the known visual auroral reports. These reports make it possible to estimate that the equatorward boundary of the auroral oval in the Eastern Hemisphere extended at least beyond the overhead positions of the Russian stations (≈37° MLAT), even during the recovery phase of the Carrington storms, after the extreme negative excursion recorded at Bombay. The conservative estimate of the equatorward boundary of auroral oval in the

Eastern Hemisphere provides further insights on the cause of this magnetic negative excursion in the context of potential auroral contributions.

Revising the spatial evolution of the auroral oval around the Carrington event, we compared the equatorward boundary of auroral oval and *Dst* value of the Carrington storms with those of the other extreme magnetic storms in February 1872, September 1909, May 1921, and March 1989. The initial comparison reveals that the Carrington event is probably not the exceptional extreme storm but one of the most extreme magnetic storms. While this event has been considered to be a once-in-a-century catastrophe, the historical observations warn us that this may be something that occurs more frequently and hence might be a more imminent threat to modern civilization.

Acknowledgments
This research was conducted under the support of the Grant-in-Aid from the Ministry of Education, Culture, Sports, Science and Technology of Japan, Grants JP15H05814 (PI: K. Ichimoto), JP18H01254 (PI: H. Isobe), and JP15H05816 (PI: S. Yoden), a Grant-in-Aid for JSPS Research Fellows JP17J06954 (PI: H. Hayakawa), and a mission project of the RISH in Kyoto University. D. J. K. was partially supported by AFOSR Grant FA9550-17-1-0258. This project has received funding from the European Union's Horizon 2020 research and innovation program under Grant Agreement 824135 (SOLARNET). We thank Michael Burton, John Butler, Sian Prosser, Marco Ferrucci, Fabrizio Giorgi, Luís São Bento, and Rui Lino for providing accesses and permissions for researches on historical manuscripts in the Armagh Observatory, the Royal Astronomical Society, INAF Observatorio Astronomico di Roma, Biblioteca Pública e Arquivo Regional João José da Graça at Horta, and Biblioteca Pública e Arquivo Regional Luís da Silva Ribeiro at Angra do Heroísmo. Data from Colaba is a reproduction of Figure 4 of Hayakawa, Ebihara, Hand, et al. (2018), as a result of the Bilateral Research Project between India (DST) and Japan (JSPS). We thank the National Library of Australia, The National Library of New Zealand, Biblioteca Nacional de Portugal, Biblioteca Pública Municipal do Porto, Biblioteca Pública de Braga, Biblioteca Dixital de Galicia, Biblioteca Nacional de España, Arxiu de Revistes Catalanes Antigues, and Hemeroteca Nacional Digital de México for letting us consult newspapers from Australia, New Zealand, Portugal, Spain, and Mexico. We thank Atsushi Soga and Tadanobu Aoyama for their advice on the interpretation of Russian meteorological records, Víctor M. S. Carrasco for providing the background data of Carrasco et al. (2016), Rainer Arlt for his helpful comments on Schwabe's sunspot observations, Lidia van Driel for her helpful comments on sunspot groups around this event, Mike A. Hapgood for his helpful comments on the contemporary magnetic measurements, Christopher J. Scott and Edward W. Cliver for his helpful comments on this article, and SILSO for providing total sunspot number series.

References

Akasofu, S.-I., & Kamide, Y. (2005). Comment on "The extreme magnetic storm of 1–2 September 1859" by B. T. Tsurutani, W. D. Gonzalez, G. S. Lakhina, and S. Alex. *Journal of Geophysical Research*, *110*, A09226. https://doi.org/10.1029/2005JA011005

Altamore, A., Poppi, F., & Bosco, T. (2018). The Rome historical Cauchoix Telescope recovered. In S. J. G. Gionti, & S. J. J. B. Kikwaya Eluo (Eds.), *The Vatican Observatory, Castel Gandolfo: 80th Anniversary Celebration*, *Astrophysics and Space Science Proceedings* (Vol. 51, pp. 185–196). Cham: Springer. https://doi.org/10.1007/978-3-319-67205-2_13

Angenheister, G., & Westland, C. J. (1921). The magnetic storm of May 13–16, 1921, at Apia Observatory, Samoa. *Terrestrial Magnetism and Atmospheric Electricity*, *26*, 30. https://doi.org/10.1029/TE026i001p00030

Arlt, R. (2011). The sunspot observations by Samuel Heinrich Schwabe. *Astronomische Nachrichten*, *332*(8), 805. https://doi.org/10.1002/asna.201111601

Arlt, R., Leussu, R., Giese, N., Mursula, K., & Usoskin, I. G. (2013). Sunspot positions and sizes for 1825–1867 from the observations by Samuel Heinrich Schwabe. *Monthly Notices of the Royal Astronomical Society*, *433*(4), 3165–3172. https://doi.org/10.1093/mnras/stt961

Baker, D. N., Li, X., Pulkkinen, A., Ngwira, C. M., Mays, M. L., Galvin, A. B., & Simunac, K. D. C. (2013). A major solar eruptive event in July 2012: Defining extreme space weather scenarios. *Space Weather*, *11*, 585–591. https://doi.org/10.1002/swe.20097

Baker, D. N., Battel, S. J., & Bennett, C. L. (2008). *Severe space weather events—Understanding societal and economic impacts*. Washington DC: National Academies Press.

Boteler, D. H. (2006). The super storms of August/September 1859 and their effects on the telegraph system. *Advances in Space Research*, *38*(2), 159–172. https://doi.org/10.1016/j.asr.2006.01.013

Butler, J., & Hoskin, M. (1987). The archives of Armagh Observatory. *Journal for the History of Astronomy*, *18*(4), 295–307. https://doi.org/10.1177/002182868701800410

Cahill, L. J. (1966). Inflation of the inner magnetosphere during a magnetic storm. *Journal of Geophysical Research*, *71*, 4505–4519. https://doi.org/10.1029/JZ071i019p04505

Carrasco, V. M. S., Vaquero, J. M., Gallego, M. C., & Sánchez-Bajo, F. A. (2016). Normalized sunspot-area series starting in 1832: An update. *Solar Physics*, *291*(9-10), 2931–2940. https://doi.org/10.1007/s11207-016-0943-9

Carrington, R. C. (1859). Description of a singular appearance seen in the Sun on September 1, 1859. *Monthly Notices of the Royal Astronomical Society*, *20*, 13–15. https://doi.org/10.1093/mnras/20.1.13

Carrington, R. C. (1863). Observations of the spots on the Sun from November 9, 1853, to March 24, 1861, made at Redhill, London.

Chapman, S. (1957a). The aurora in middle and low latitudes. *Nature*, *179*(4549), 7–11. https://doi.org/10.1038/179007a0

Chapman, S. (1957b). Auroral Observations in India and Pakistan. *Bulletin of the National Institute of Science of India*, *9*, 180–192.

Cid, C., Palacios, J., Saiz, E., Guerrero, A., & Cerrato, Y. (2014). On extreme geomagnetic storms. *Journal of Space Weather and Space Climate*, *4*, A28. https://doi.org/10.1051/swsc/2014026

Cid, C., Saiz, E., Guerrero, A., Palacios, J., & Cerrato, Y. (2015). A Carrington-like geomagnetic storm observed in the 21st century. *Journal of Space Weather and Space Climate*, *5*, A16. https://doi.org/10.1051/swsc/2015017

Clette, F., & Lefèvre, L. (2016). The new sunspot number: Assembling all corrections. *Solar Physics*, *291*(9-10), 2629–2651. https://doi.org/10.1007/s11207-016-1014-y

Clette, F., Svalgaard, L., Vaquero, J. M., & Cliver, E. W. (2014). Revisiting the sunspot number. A 400-year perspective on the solar cycle. *Space Science Reviews*, *186*(1-4), 35–103. https://doi.org/10.1007/s11214-014-0074-2

Cliver, E. W. (2006). The 1859 space weather event: Then and now. *Advances in Space Research*, *38*(2), 119–129. https://doi.org/10.1016/j.asr.2005.07.077

Cliver, E. W., & Dietrich, W. F. (2013). The 1859 space weather event revisited: Limits of extreme activity. *Journal of Space Weather and Space Climate*, *3*, A31. https://doi.org/10.1051/swsc/2013053

Cliver, E. W., & Keer, N. C. (2012). Richard Christopher Carrington: Briefly among the great scientists of his time. *Solar Physics*, *280*(1), 1–31. https://doi.org/10.1007/s11207-012-0034-5

Cliver, E. W., & Svalgaard, L. (2004). The 1859 solar-terrestrial disturbance and the current limits of extreme space weather activity. *Solar Physics*, *224*(1-2), 407–422. https://doi.org/10.1007/s11207-005-4980-z

Crookes, W. (1859). *The photographic news* (Vol. 3). London: Cassell, Petter, and Galpin.

Curto, J. J., Castell, J., & del Moral, F. (2016). Sfe: Waiting for the big one. *Journal of Space Weather and Space Climate*, *6*, A23. https://doi.org/10.1051/swsc/2016018

Daglis, I. A. (Ed) (2001). *Space storms and space weather hazards*, *NATO Science Series, Ser. II* (Vol. 38). Dordrecht: Kluwer.

Daglis, I. A., Thorne, R. M., Baumjohann, W., & Orsini, S. (1999). The terrestrial ring current: Origin, formation, and decay. *Reviews of Geophysics*, *37*(4), 407–438. https://doi.org/10.1029/1999RG900009

Dyer, C., Hands, A., Ryden, K., & Lei, F. (2018). Extreme atmospheric radiation environments and single event effects. *IEEE Transactions on Nuclear Science*, *65*(1), 432–438. https://doi.org/10.1109/TNS.2017.2761258

Ebihara, Y., Hayakawa, H., Iwahashi, K., Tamazawa, H., Kawamura, A. D., & Isobe, H. (2017). Possible cause of extremely bright aurora witnessed in East Asia on 17 September 1770. *Space Weather*, *15*, 1373–1382. https://doi.org/10.1002/2017SW001693

Farrona, A. M., Gallego, M.-C., Vaquero, J. M., & Dominguez-Castro, F. (2011). Spanish eyewitness accounts of the great space weather event of 1859. *Acta Geodaetica et Geophysica Hungarica*, *46*(3), 370–377. https://doi.org/10.1556/AGeod.46.2011.3.7

Gannon, J. L., & Love, J. J. (2011). USGS 1-min Dst index. *Journal of Atmospheric and Solar-Terrestrial Physics*, *73*(2–3), 323–334. https://doi.org/10.1016/j.jastp.2010.02.013

Gnevyshev, M. N. (1963). The corona and the 11-year cycle of solar activity. *Soviet Astronomy*, *7*, 311–318.

Gonzalez, W. D., Echer, E., Tsurutani, B. T., Clúa de Gonzalez, A. L., & Dal Lago, A. (2011). Interplanetary origin of intense, superintense and extreme geomagnetic storms. *Space Science Reviews*, *158*(1), 69–89. https://doi.org/10.1007/s11214-010-9715-2

González-Esparza, J. A., & Cuevas-Cardona, M. C. (2018). Observations of low-latitude red aurora in Mexico during the 1859 Carrington geomagnetic storm. *Space Weather*, *16*, 593–600. https://doi.org/10.1029/2017SW001789

Gopalswamy, N., Lara, A., Manoharan, P. K., & Howard, R. A. (2005). An empirical model to predict the 1-AU arrival of interplanetary shocks. *Advances in Space Research*, *36*(12), 2289–2294. https://doi.org/10.1016/j.asr.2004.07.014

Gopalswamy, N., Xie, H., Yashiro, S., Akiyama, S., Mäkelä, P., & Usoskin, I. G. (2012). Properties of ground level enhancement events and the associated solar eruptions during solar cycle 23. *Space Science Reviews*, *171*(1-4), 23–60. https://doi.org/10.1007/s11214-012-9890-4

Green, J. L., & Boardsen, S. (2006). Duration and extent of the great auroral storm of 1859. *Advances in Space Research*, *38*(2), 130–135. https://doi.org/10.1016/j.asr.2005.08.054

Green, J. L., Boardsen, S., Odenwald, S., Humble, J., & Pazamickas, K. A. (2006). Eyewitness reports of the great auroral storm of 1859. *Advances in Space Research*, *38*(2), 145–154. https://doi.org/10.1016/j.asr.2005.12.021

Hapgood, M. (2019). The great storm of May 1921: An exemplar of a dangerous space weather event. *Space Weather*, *17*, 950–975. https://doi.org/10.1029/2019SW002195

Hapgood, M. A. (2011). Towards a scientific understanding of the risk from extreme space weather. *Advances in Space Research*, *47*(12), 2059–2072. https://doi.org/10.1016/j.asr.2010.02.007

Hayakawa, H., Ebihara, Y., Cliver, E. W., Hattori, K., Toriumi, S., Love, J. J., et al. (2019). The extreme space weather event in September 1909. *Monthly Notices of the Royal Astronomical Society*, *484*(3), 4083–4099. https://doi.org/10.1093/mnras/sty3196

Hayakawa, H., Ebihara, Y., Hand, D. P., Hayakawa, S., Kumar, S., Mukherjee, S., & Veenadhari, B. (2018). Low-latitude aurorae during the extreme space weather events in 1859. *The Astrophysical Journal*, *869*, 57. https://doi.org/10.3847/1538-4357/aae47c

Hayakawa, H., Ebihara, Y., Willis, D. M., Hattori, K., Giunta, A. S., Wild, M. N., et al. (2018). The great space weather event during 1872 February recorded in East Asia. *The Astrophysical Journal*, *862*(1), 15. https://doi.org/10.3847/1538-4357/aaca40

Hayakawa, H., Iwahashi, K., Ebihara, Y., Tamazawa, H., Shibata, K., Knipp, D. J., et al. (2017). Long-lasting extreme magnetic storm activities in 1770 found in historical documents. *The Astrophysical Journal Letters*, *850*(2), L31. https://doi.org/10.3847/2041-8213/aa9661

Hayakawa, H., Iwahashi, K., Tamazawa, H., Isobe, H., Kataoka, R., Ebihara, Y., et al. (2016). East Asian observations of low-latitude aurora during the Carrington magnetic storm, East Asian observations of low-latitude aurora during the Carrington magnetic storm. *Publications of the Astronomical Society of Japan*, *68*(6), 99. https://doi.org/10.1093/pasj/psw097

Hayakawa, H., Willis, D. M., Hattori, K., Notsu, Y., Wild, M. N., & Karoff, C. (2019). Unaided-eye sunspot observations in 1769 November: A comparison of graphical records in the East and the West. *Solar Physics*, *294*, 95. https://doi.org/10.1007/s11207-019-1488-5

Heis, E. (1859). *Wochenschrift für Astronomie, Meteorologie und Geographie* (Vol. 2). Halle: H. W. Schmidt.

Heis, E. (1860). *Wochenschrift für Astronomie, Meteorologie und Geographie* (Vol. 3). Halle: H. W. Schmidt.

Heis, E. (1861). *Wochenschrift für Astronomie, Meteorologie und Geographie* (Vol. 4). Halle: H. W. Schmidt.

Henwood, R., Chapman, S. C., & Willis, D. M. (2010). Increasing lifetime of recurrent sunspot groups within the Greenwich photoheliographic results. *Solar Physics*, *262*(2), 299–313. https://doi.org/10.1007/s11207-009-9419-5

Hodgson, R. (1859). On a curious appearance seen in the Sun. *Monthly Notices of the Royal Astronomical Society*, *20*, 15–16. https://doi.org/10.1093/mnras/20.1.15

Humble, J. E. (2006). The solar events of August/September 1859—Surviving Australian observations. *Advances in Space Research*, *38*(2), 155–158. https://doi.org/10.1016/j.asr.2005.08.053

Jackson, A., Jonkers, A. R. T., & Walker, M. R. (2000). Four centuries of geomagnetic secular variation from historical records. *Philosophical Transactions of the Royal Society of London*, *358*(1768), 957. https://doi.org/10.1098/rsta.2000.0569

Johnson, M. J. (1857). Address delivered by the President, M. J. Johnson, Esq., on presenting the Medal of the Society to M. Schwabe. *Monthly Notices of the Royal Astronomical Society*, *17*, 126–132. https://doi.org/10.1093/mnras/17.4.126

Jones, H. S. (1955). *Sunspot and geomagnetic storm data*. London: Her Majesty's Stationary Office.

Keika, K., Ebihara, Y., & Kataoka, R. (2015). What caused the rapid recovery of the Carrington storm? *Earth, Planets and Space*, *67*, 65. https://doi.org/10.1186/s40623-015-0217-z

Kimball, D.S. (1960). A study of the aurora of 1859. Sci. Rep. No. 6, University of Alaska, No. 6.

Knipp, D. J., Fraser, B. J., Shea, M. A., & Smart, D. F. (2018). On the little-known consequences of the 4 August 1972 ultra-fast coronal mass ejecta: Facts, commentary, and call to action. *Space Weather*, *16*, 1635–1643. https://doi.org/10.1029/2018SW002024

Kumar, S., Veenadhari, B., Ram, S. T., Selvakumaran, R., Mukherjee, S., Singh, R., & Kadam, B. D. (2016). Estimation of interplanetary electric field conditions for historical geomagnetic storms. *Journal of Geophysical Research: Space Physics*, *120*, 7307–7317. https://doi.org/10.1002/2015JA021661

Kupffer, A. (1860). Annales de l'observatoire physique central de Russie – Année 1859.

Lakhina, G. S., Alex, S., Tsurutani, B. T., & Gonzalez, W. D. (2013). Supermagnetic storms: Hazard to society. In A. S. Sharma, A. Bunde, V. P. Dimri, & D. N. Baker (Eds.), *Extreme events and natural hazards: The complexity perspective* (Vol. 4, No. 2, pp. 267–278). https://doi.org/10.1029/2011GM001073

Lakhina, G. S., & Tsurutani, B. T. (2017). Supermagnetic storms: Past, present, and future. In N. Buzulukova (Ed.), *Extreme events in geospace* (pp. 157–185). Amsterdam: Elsevier. https://doi.org/10.1016/B978-0-12-812700-1.00007-8

Lefèvre, L., Vennerstrøm, S., Dumbović, M., Vršnak, B., Sudar, D., Arlt, R., et al. (2016). Detailed analysis of solar data related to historical extreme geomagnetic storms: 1868–2010. *Solar Physics*, *291*(5), 1483–1531. https://doi.org/10.1007/s11207-016-0892-3

Li, X., Temerin, M., Tsurutani, B. T., & Alex, S. (2006). Modeling of 1–2 September 1859 super magnetic storm. *Advances in Space Research*, *38*(2), 273–279. https://doi.org/10.1016/j.asr.2005.06.070

Liu, Y. D., Luhmann, J. G., Kajdič, P., Kilpua, E. K. J., Lugaz, N., Nitta, N. V., et al. (2014). Observations of an extreme storm in interplanetary space caused by successive coronal mass ejections. *Nature Communications*, *5*(1), 3481. https://doi.org/10.1038/ncomms4481

Liu, Y. D., Zhao, X., Hu, H., Vourlidas, A., & Zhu, B. (2019). A comparative study of 2017 July and 2012 July complex eruptions: Are solar superstorms "perfect storms" in nature? *The Astrophysical Journal Supplement Series*, *241*(2), 15. https://doi.org/10.3847/1538-4365/ab0649

Love, J. J., Hayakawa, H., & Cliver, E. W. (2019a). On the intensity of the magnetic superstorm of September 1909. *Space Weather*, *17*, 37–45 . https://doi.org/10.1029/2018SW002079

Love, J. J., Hayakawa, H., & Cliver, E. W. (2019b). Intensity and impact of the New York Railroad superstorm of May 1921. *Space Weather*, *17*. https://doi.org/10.1029/2019SW002250

McCracken, K. G., Dreschhoff, G. A. M., Zeller, E. J., Smart, D. F., & Shea, M. A. (2001). Solar cosmic ray events for the period 1561–1994: 1. Identification in polar ice, 1561–1950. *Journal of Geophysical Research*, *106*(A10), 21,585–21,598. https://doi.org/10.1029/2000JA000237

McIntosh, P. S. (1990). The classification of sunspot groups. *Solar Physics*, *125*, 251–267. https://doi.org/10.1007/BF00158405

Mekhaldi, F., McConnell, J. R., Adolphi, F., Arienzo, M. M., Chellman, N. J., Maselli, O. J., et al. (2018). No coincident nitrate enhancement events in polar ice cores following the largest known solar storms. *Journal of Geophysical Research: Atmospheres*, *122*, 11,900–11,913. https://doi.org/10.1002/2017JD027325

Moreno Cárdenas, F., Cristancho Sánchez, S., & Vargas Domínguez, S. (2016). The grand aurorae borealis seen in Colombia in 1859. *Advances in Space Research*, *57*(1), 257–267. https://doi.org/10.1016/j.asr.2015.08.026

Namekata, K., Maehara, H., Notsu, Y., Toriumi, S., Hayakawa, H., Ikuta, K., et al. (2019). Lifetimes and emergence/decay rates of star spots on solar-type stars estimated by Kepler data in comparison with those of sunspots. *The Astrophysical Journal*, *871*(2), 187. https://doi.org/10.3847/1538-4357/aaf471

Neidig, D. F., & Cliver, E. W. (1983). A catalog of solar white-light flares, including their statistical properties and associated emissions, 1859–1982, AFGL Technical Report.

Neumeyer, G. (1864). *Meteorological and nautical taken in the colony of Victoria*. Melbourne: Ferres.

Nevanlinna, H. (2006). A study on the great geomagnetic storm of 1859: Comparisons with other storms in the 19th century. *Advances in Space Research*, *38*(2), 180–187. https://doi.org/10.1016/j.asr.2005.07.076

Nevanlinna, H. (2008). On geomagnetic variations during the August–September storms of 1859. *Advances in Space Research*, *42*(1), 171–180. https://doi.org/10.1016/j.asr.2008.01.002

Ngwira, C. M., Pulkkinen, A., Leila Mays, M., Kuznetsova, M. M., Galvin, A. B., Simunac, K., et al. (2013). Simulation of the 23 July 2012 extreme space weather event: What if this extremely rare CME was Earth directed? *Space Weather*, *11*, 671–679. https://doi.org/10.1002/2013SW000990

Nishida, A. (1968). Coherence of geomagnetic DP 2 fluctuations with interplanetary magnetic variations. *Journal of Geophysical Research*, *73*(17), 5549–5559. https://doi.org/10.1029/JA073i017p05549

O'Brien, B. J., Laughlin, C. D., Van Allen, J. A., & Frank, L. A. (1962). Measurements of the intensity and spectrum of electrons at 1000-kilometer altitude and high latitudes. *Journal of Geophysical Research*, *67*, 1209–1225. https://doi.org/10.1029/JZ067i004p01209

Ribeiro, P., Vaquero, J. M., & Trigo, R. M. (2011). Geomagnetic records of Carrington's storm from Guatemala. *Journal of Atmospheric and Solar-Terrestrial Physics*, *73*, 308–315. https://doi.org/10.1016/j.jastp.2009.12.017

Rich, F. J., & Denig, W. F. (1992). The major magnetic storm of March 13–14, 1989 and associated ionosphere effects. *Canadian Journal of Physics*, *70*(7), 510–525. https://doi.org/10.1139/p92-086

Riley, P. (2012). On the probability of occurrence of extreme space weather events. *Space Weather*, *10*, S02012. https://doi.org/10.1029/2011SW000734

Riley, P., Baker, D., Liu, Y. D., Verronen, P., Singer, H., & Güdel, M. (2018). Extreme space weather events: From cradle to grave. *Space Science Reviews*, *214*(1), 21. https://doi.org/10.1007/s11214-017-0456-3

Riley, P., & Love, J. J. (2017). Extreme geomagnetic storms: Probabilistic forecasts and their uncertainties. *Space Weather*, *15*, 53–64. https://doi.org/10.1002/2016SW001470

Rubenson, R. (1879). Catalogue des aurores boreales observes en Suede, Kungl. Sv. Vetenskapsakad. *Mandl*, *15*, 3–184.

Rubenson, R. (1882) Catalogue des aurores boreales observees en Suede, Kungl. Sv. Vetenskapsakad. *Handl*, *18*, 1–300.

Schrijver, C. J., Beer, J., Baltensperger, U., Cliver, E. W., Güdel, M., Hudson, H. S., et al. (2012). Estimating the frequency of extremely energetic solar events, based on solar, stellar, lunar, and terrestrial records. *Journal of Geophysical Research*, *117*, A08103. https://doi.org/10.1029/2012JA017706

Secchi, A. (1859). Observationes des taches et facules du soleil á l'Observatoire du collége Romain. *Comptes Rendus*, *49*, 191–194.

Secchi, A. (1860). *Memorie dell'osservatorio del Collegio Romano* (Vol. 2). Rome: Osservatorio del Collegio romano.

Shea, M. A., Smart, D. F., McCracken, K. G., Dreschhoff, G. A. M., & Spence, H. E. (2006). Solar proton events for 450 years: The Carrington event in perspective. *Advances in Space Research*, *38*(2), 232–238. https://doi.org/10.1016/j.asr.2005.02.100

Shiokawa, K., Baumjohann, W., Haerendel, G., Paschmann, G., Fennell, J. F., Friis-Christensen, E., et al. (1998). High-speed ion flow, substorm current wedge, and multiple Pi 2 pulsations. *Journal of Geophysical Research*, *103*(A3), 4491–4508. https://doi.org/10.1029/97JA01680 Silverman, S. M. (1995). Low latitude auroras: the storm of 25 September 1909. *Journal of Atmospheric and Terrestrial Physics*, *57*(6), 673–685. https://doi.org/10.1016/0021-9169(94)E0012-C

Silverman, S. M. (1998). Early auroral observations. *Journal of Atmospheric and Solar-Terrestrial Physics*, *60*(10), 997–1006. https://doi.org/10.1016/S1364-6826(98)00040-6

Silverman, S. M. (2006). Comparison of the aurora of September 1/2, 1859 with other great auroras. *Advances in Space Research*, *38*(2), 136–144. https://doi.org/10.1016/j.asr.2005.03.157

Silverman, S. M. (2008). Low-latitude auroras: The great aurora of 4 February 1872. *Journal of Atmospheric and Solar-Terrestrial Physics*, *70*(10), 1301–1308. https://doi.org/10.1016/j.jastp.2008.03.012

Silverman, S. M., & Cliver, E. W. (2001). Low-latitude auroras: The magnetic storm of 14–15 May 1921. *Journal of Atmospheric and Solar-Terrestrial Physics*, *63*(5), 523–535. https://doi.org/10.1016/S1364-6826(00)00174-7

Siscoe, G., Crooker, N. U., & Clauer, C. R. (2006). Dst of the Carrington storm of 1859. *Advances in Space Research*, *38*(2), 173–179. https://doi.org/10.1016/j.asr.2005.02.102

Smart, D. F., Shea, M. A., & McCracken, K. G. (2006). The Carrington event: Possible solar proton intensity time profile. *Advances in Space Research*, *38*(2), 215–225. https://doi.org/10.1016/j.asr.2005.04.116

Stewart, B. (1861). On the great magnetic disturbance which extended from August 28 to September 7, 1859, as recorded by photography at the Kew Observatory. *Philosophical Transactions of the Royal Society of London*, *151*, 423–430.

Storini, M., Bazilevskaya, G. A., Fluckiger, E. O., Krainev, M. B., Makhmutov, V. S., & Sladkova, A. I. (2003). The GNEVYSHEV gap: A review for space weather. *Advances in Space Research*, *31*(4), 895–900. https://doi.org/10.1016/s0273-1177(02)00789-5

Sugiura, M. (1964). *Hourly value of equatorial Dst for the IGY*, *Ann. Int. Geophys. Year* (Vol. 35, pp. 9–45). Oxford: Pergamon Press.

Sugiura, M., & Kamei, T. (1991). *Equatorial Dst index 1957–1986*, *IAGA Bull.* (Vol. 40). Saint-Maur-des-Fossess, France: ISGI Publication Office.

Thébault, E., Finlay, C. C., Beggan, C. D., Alken, P., Aubert, J., Barrois, O., et al. (2015). International Geomagnetic Reference Field: The 12th generation. *Earth, Planets and Space*, *67*(1), 79. https://doi.org/10.1186/s40623-015-0228-9

Thomson, N. R., Rodger, C. J., & Dowden, R. L. (2004). Ionosphere gives size of greatest solar flare. *Geophysical Research Letters*, *31*, L06803. https://doi.org/10.1029/2003GL019345

Toriumi, S., Schrijver, C. J., Harra, L. K., Hudson, H., & Nagashima, K. (2017). Magnetic properties of solar active regions that govern large solar flares and eruptions. *The Astrophysical Journal*, *834*(1), 56. https://doi.org/10.3847/1538-4357/834/1/56

Toriumi, S., & Wang, H. (2019). Flare-productive active regions. *Living Reviews in Solar Physics*, *16*, 3. https://doi.org/10.1007/s41116-019-0019-7

Trombolt, S. (1902). *Katalog der in Norwegen his Juni 1878 beobachteten Nordlichier*. Bragger, Oslo. Tsurutani, B. T., Gonzalez, W. D., Lakhina, G. S., & Alex, S. (2003). The extreme magnetic storm of 1–2 September 1859. *Journal of Geophysical Research*, *108*(A7), 1268. https://doi.org/10.1029/2002JA009504

Usoskin, I. G. (2017). A history of solar activity over millennia. *Living Reviews in Solar Physics*, *14*(1), 3. https://doi.org/10.1007/s41116-017-0006-9

Usoskin, I. G., & Kovaltsov, G. A. (2012). Occurrence of extreme solar particle events: Assessment from historical proxy data. *The Astrophysical Journal*, *757*(1), 92. https://doi.org/10.1088/0004-637X/757/1/92

Vaquero, J. M., & Vázquez, M. (2009). *The Sun recorded through history: Scientific data extracted from historical documents*. Berlin: Springer.

Vaquero, J. M., Vázquez, M., & Sánchez Almeida, J. (2017). Evidence of a white-light flare on 10 September 1886. *Solar Physics*, *292*(2), 33. https://doi.org/10.1007/s11207-017-1059-6

Veselovsky, I. S., Mursula, K., Ptitsyna, N. G., Tyasto, M. I., & Yakovchouk, O. S. (2009). Sporadic and recurrent geomagnetic disturbances in 1859–1860 according to the archived data from the Russian network of stations. *Geomagnetism and Aeronomy*, *49*, 163. https://doi.org/10.1134/S0016793209020042

Willis, D. M., Stephenson, F. R., & Fang, H. (2007). Sporadic aurorae observed in East Asia. *Annales Geophysicae*, *25*(2), 417–436. https://doi.org/10.5194/angeo-25-417-2007

Wolff, E. W., Bigler, M., Curran, M. A. J., Dibb, J. E., Frey, M. M., Legrand, M., & McConnell, J. R. (2012). The Carrington event not observed in most ice core nitrate records. *Geophysical Research Letters*, *39*, L08503. https://doi.org/10.1029/2012GL051603

Yokoyama, N., Kamide, Y., & Miyaoka, H. (1998). The size of the auroral belt during magnetic storms. *Annales Geophysicae*, *16*(5), 566–573. https://doi.org/10.1007/s00585-998-0566-z

Zirin, H., & Liggett, M. A. (1987). Delta spots and great flares. *Solar Physics*, *113*(1-2), 267–283. https://doi.org/10.1007/BF00147707